Available online at www.sciencedirect.com
SCIENCE DIRECT
Journal of Photochemistry and Photobiology A: Chemistry 177 (2006) 68–75
Journal of Photochemistry and Photobiology A:Chemistry
www.elsevier.com/locate/jphotochem

Atomic layer deposition of $TiO_{2-x}N_x$ thin films for photocatalytic applications

Viljami Pore [a,*], Mikko Heikkilä [a], Mikko Ritala [a], Markku Leskelä [a], Sami Areva [b]

[a] *Department of Chemistry, University of Helsinki, P.O. Box 55, FI-00014 Helsinki, Finland*
[b] *Department of Physical Chemistry, Åbo Akademi University, Porthansgatan 3-5, FI-20500 Turku, Finland*

Received 3 January 2005; received in revised form 20 April 2005; accepted 11 May 2005
Available online 13 June 2005

Abstract

Titanium dioxide (TiO_2) is recognized as the most efficient photocatalytic material, but due to its large band gap energy it can only be excited by UV irradiation. Doping TiO_2 with nitrogen is a promising modification method for the utilization of visible light in photocatalysis. In this work, nitrogen-doped TiO_2 films were grown by atomic layer deposition (ALD) using $TiCl_4$, NH_3 and water as precursors. All growth experiments were done at 500 °C. The films were characterized by XRD, XPS, SEM and UV–vis spectrometry. The influence of nitrogen doping on the photocatalytic activity of the films in the UV and visible light was evaluated by the degradation of a thin layer of stearic acid and by linear sweep voltammetry. Light-induced superhydrophilicity of the films was also studied. It was found that the films could be excited by visible light, but they also suffered from increased recombination.

Keywords: Photocatalysis; Titanium dioxide; Nitrogen doping; ALD; Thin films

1. Introduction

Since the discovery of the photocatalytic properties of titanium dioxide (TiO_2) in the 70s, there has been a tremendous amount of scientific interest on the subject [1]. More recently, many commercial products based on photocatalysis have been appearing on the market and hundreds of patent applications are filed every year. Even though anatase TiO_2 is recognized as the most efficient photocatalytic material, it has one significant limitation. Due to its large band gap energy of 3.2 eV, it requires UV light for the photocatalytic reactions to happen. For better utilization of indoor and outdoor lighting, several modifications of TiO_2 have been attempted. These include oxygen deficient TiO_2 [2], composite materials with a smaller band gap semiconductor [3,4] and cation-doped TiO_2 [5–7] or anion-doped TiO_2 [8–11]. Doping with nitrogen is one of the most promising ways of achieving visible light activity in TiO_2 and good results have been obtained by several research groups [8,12–17]. Preparative routes for nitrogen-doped TiO_2 powders include oxidative annealing of TiN [18], annealing of TiO_2 in gaseous ammonia [8,12] and various solution-based methods [13–15]. For thin films, sputtering [8,19–21] and pulsed laser deposition [17] in N_2-containing atmosphere and annealing TiO_2 in gaseous ammonia [16] have been used.

Atomic layer deposition (ALD) is a gas-phase thin film deposition method based on alternate saturative surface reactions [22,23]. The precursor vapours are pulsed into the reactor one at a time and separated by purging with an inert gas. During each precursor pulse, the surface becomes saturated with the precursor in question. This results in a self-limiting film growth mechanism proceeding in a stepwise manner which has many advantages. These include good reproducibility, excellent conformality and uniformity over the whole substrate area, and accurate control of film

* Corresponding author. Tel.: +358 9 191 50208; fax: +358 9 191 50198.
E-mail address: viljami.pore@helsinki.fi (V. Pore).

1010-6030/$ – see front matter © 2005 Elsevier B.V. All rights reserved.
doi:10.1016/j.jphotochem.2005.05.013

thickness and composition. In an ideal ALD process the film thickness depends solely on the number of deposition cycles and the composition can be controlled by varying the pulsing sequence of the desired precursors. These characteristic features of ALD are all very practical in designing and preparing photocatalytic thin films. The excellent film conformality enables one to deposit a film of equal thickness on very high aspect ratio and large-surface area substrates. Even porous powders have been coated by ALD [24]. Also, the accurate control of film composition should make ALD a powerful tool in preparing different kinds of doped and composite photocatalyst thin films.

Several studies have been published about the deposition of TiO_2 films by ALD [25–29]. Titanium alkoxides and halides are typically used as titanium precursors and H_2O and H_2O_2 as oxygen sources. The deposition of TiN films from titanium halides and NH_3 has also been described [30–31]. In this work, nitrogen-doped TiO_2 films were deposited by combining the TiN and TiO_2 ALD processes with $TiCl_4$ as the titanium precursor [25,30]. The deposition sequence consisted of two repeating cycles. During the first cycle a thin layer of TiN was grown from $TiCl_4$ and NH_3. In the second cycle TiO_2 was deposited from $TiCl_4$ and H_2O. During this second cycle the TiN layer underneath was also oxidized to TiO_2. This oxidation was not complete however, and some nitrogen was left in the films leading to $TiO_{2-x}N_x$. By varying the relative amounts of TiN and TiO_2 deposition cycles, $TiO_{2-x}N_x$ films with different nitrogen concentrations were produced.

2. Experimental

The films were deposited onto 5 cm × 5 cm borosilicate glass and indium tin oxide (ITO)-coated glass substrates in a flow-type F-120 ALD reactor (ASM Microchemistry Oy, Helsinki, Finland) [32]. The reactor was operated under a pressure of about 10 mbar using nitrogen (made on site by a Nitrox UHPN 3000 generator, rated purity of 99.9995%) as a carrier and purging gas. $TiCl_4$ (99.9%, Aldrich), NH_3 (99.999%, Oy Aga Ab) and H_2O were used as the precursors. $TiCl_4$ was evaporated from an external reservoir thermostated to 21 °C and pulsed with solenoid valves. H_2O and NH_3 were in external reservoirs at room temperature and led into the reactor through needle and solenoid valves.

Film compositions were obtained by X-ray photoelectron spectroscopy (XPS) using a Physical Electronics Quantum 2000 instrument equipped with a monochromatic Al Kα X-ray source. Operating power was 25 W and the spot diameter 100 μm. An electron flood gun and a low energy ion gun were used for charge compensation. The detector position was at an angle of 45° in relation to the sample surface. XPS depth profiling was carried out with Ar^+ ion sputtering. Focused beam with a current of 50 μA, raster area of 2 mm × 2 mm and an acceleration voltage of 4 kV were employed. Surface concentrations were determined with MultiPak 6.0 software using peak areas and relative sensitivity factors to give surface concentrations in atomic percent. Transmittance spectra were measured with a Hitachi U-2000 spectrophotometer in a wavelength range of 190–1100 nm. Film thicknesses and refractive indices were determined by fitting [33] transmittance spectra in a wavelength range of 400–1100 nm. Band gap values were estimated according to Swanepoel [34]. Film crystallinity was examined with a Bruker D8 Advance X-ray diffractometer at grazing incidence mode with an incident angle of 1° using Cu Kα radiation. θ–2θ scans were performed with a Philips MPD 1880 powder X-ray diffractometer. Film morphology was examined with a Hitachi S4800 field emission scanning electron microscope using an acceleration voltage of 1.0 kV.

Photocatalytic degradation measurements were performed on a solid layer of stearic acid ($CH_3(CH_2)_{16}CO_2H$, Aldrich, 95%). UV illumination was done with an 18-W Sylvania Blacklight Blue UV lamp that emits at wavelengths 340–410 nm with a peak maximum at 365 nm. The UV irradiance on the film surface was measured to be 1.1 mW/cm^2 (HD9021 radiometer, Delta Ohm). An 18-W fluorescent lamp (Airam, warm white) with a 405-nm cut-off filter (Edmund Optics, T39-427) was used as the visible light source. Before stearic acid coating all the samples were held under UV light for 3 h to photocatalytically clean the surface of any organic contaminants that might have been adsorbed from the atmosphere. Immediately after this, the stearic acid layer was dispersed on the TiO_2 surface by spin coating (P6204 Spin Coater, Specialty Coating Systems). Stearic acid was dissolved into methanol (8.8×10^{-3} M) and 200 μl of this solution was dropped on the central part of the sample, followed by 2 min rotation with a speed of 1000 rpm. The change in stearic acid layer thickness was monitored by measuring infrared absorption spectrum in a transmission mode by Perkin-Elmer Spectrum GX FTIR instrument. The absorbance of the asymmetric C–H stretching mode of the CH_2 group at the peak wavenumber 2917 cm^{-1} was converted into a thickness on the basis of an earlier observation that an absorbance of 0.01 corresponds to a thickness of 12.5 nm [35]. Water contact angles were measured by the sessile drop method (CAM 100, KSV Instruments).

Photoelectrochemical measurements were performed on an Autolab PGSTAT20 potentiostat using a three-electrode setup. The reference and counter electrodes were Ag/AgCl/3 M KCl and platinum, respectively. A nitrogen-doped TiO_2 film grown on an ITO substrate was used as the working electrode with an active area of ∼20 cm^2. Seventy milliliters of 0.1 M KCl aqueous solution was used as the electrolyte. The sample was irradiated through the substrate with chopped (7 s on/7 s off) visible light and the current density as a function of applied voltage was measured. The scanning speed was 5 mV/s. In all photoelectrochemical measurements, a 50-W halogen lamp (Philips) with a 435 nm cut-off filter (Edmund Optics, GG 435) was used as the visible light source.

3. Results and discussion

3.1. Film growth

Before the preparation of nitrogen-doped samples, pure TiO_2 and TiN films were grown from $TiCl_4$ and H_2O and $TiCl_4$ and NH_3, respectively. The TiO_2 film consisted of a mixture of anatase and rutile phases and the TiN film was determined to be cubic TiN by XRD analyses. The nitrogen-doped TiO_2 films were deposited by combining these two processes. Table 1 describes the deposition sequences used. The film thicknesses and growth rates are also shown. In all depositions the pulse/purge lengths were 0.4/0.5 s for $TiCl_4$ and H_2O and 0.5/0.3 s for NH_3. The difference between films A1–A4 and A5 is that films A1–A4 were grown by alternating TiN and TiO_2 deposition cycles, whereas film A5 was deposited by growing a thin layer of TiN followed by oxidation with water. Because TiN has a much lower growth rate than TiO_2, the growth rate of the nitrogen-doped films decreased as the relative amount of TiN pulses increased.

In an attempt to improve charge separation a two-layered film (sample B) was also deposited, where a film prepared in the same way as sample A4 was covered by a thin layer (∼25 nm) of undoped TiO_2. In addition, a nitrogen-doped film with a graded composition was grown (sample C). The film was deposited with a sequence where the TiN:TiO_2 pulsing ratio was varied gradually during deposition from 10:1 to 1:10. A thin undoped layer of TiO_2 was grown on top of this sample also.

For reference, two nitrogen-doped TiO_2 films were also prepared by annealing TiN films in air at 500 °C for 1 and 5 h (samples TiN1h and TiN5h). According to Morikawa [18], the oxidative annealing of TiN produces rutile $TiO_{2-x}N_x$.

Table 1
Deposition sequences, optically determined film thicknesses and growth rates of all the films studied

Sample	Deposition sequence[a]	Film thickness (nm)	Growth rate[c] (Å/cycle)
A1	$600 \times (X + 5Y)$	160	0.44
A2	$1000 \times (X + 3Y)$	170	0.43
A3	$2500 \times (X + Y)$	176	0.35
A4	$1500 \times (3X + Y)$	215	0.36
A5	$800 \times (5X + H_2O/\text{purge})$	121	0.30
B	$1400 \times (3X + Y) + 400 \times Y$	225	0.38
C	5000 cycles from $(10X + Y)$ to $(X + 10Y)$[b] $+ 220 \times Y$	184	0.37
TiO_2	$2000 \times Y$	90	0.45
TiN	$6000 \times X$	102 (calculated)	0.17 [30]
TiN1h	TiN annealed in air at 500 °C for 1 h		–
TiN5h	TiN annealed in air at 500 °C for 5 h		–

[a] $X = (TiCl_4/\text{purge}/NH_3/\text{purge})$, $Y = (TiCl_4/\text{purge}/H_2O/\text{purge})$.
[b] X:Y ratio decreased linearly from 10:1 to 1:10. The overall amount of X and Y cycles was 5000.
[c] Growth rates were calculated by dividing the thicknesses by the total number of $TiCl_4$ pulses. For TiN, a literature value was used.

Table 2
Nitrogen concentrations measured by XPS and estimated band gap energies of the nitrogen-doped TiO_2 films

Sample	Nitrogen concentration (at.%)	Band gap energy (eV)
A1	0.9	3.3
A2	0.7	3.3
A3	0.8	3.4
A4	3.8	3.1
A5	8.1	2.9

3.2. Characterization

The nitrogen concentrations of samples A1–A5 were determined by XPS and are listed in Table 2. The N 1s XPS spectra revealed that nitrogen in samples A1 and A2 was completely in the form of molecularly chemisorbed N_2 (peak at 401 eV) [36]. This indicates that in these samples virtually all TiN was oxidized to TiO_2 during growth. In samples A4 and A5 the binding energy of nitrogen was significantly lower (peak at 395 eV) indicating the presence of Ti–N bonding. In these films nitrogen was thus located at substitutional sites which resulted from incomplete oxidation of TiN during growth. Sample A3 had approximately an equal amount of both of these types of nitrogen present. The atomic formula of sample A3 would thus be $TiO_{1.988}N_{0.012}$, if only the N 1s peak at 395 eV was used. This is quite close to other reported visible light active $TiO_{2-x}N_x$ photocatalysts [8,12].

XPS depth profiling was performed on samples B and C (Fig. 1). Preferential sputtering of oxygen during depth profiling distorted the atomic concentrations slightly but the location of nitrogen can still be seen clearly. Sample B had a 200-nm layer with a nitrogen concentration of about 4 at.% which decreased to below 1 at.% in the ∼25 nm thick surface layer. Sample C had a graded composition near the substrate of approximately 60 nm in thickness where the nitrogen concentration changed from 10 to 1 at.%. The nitrogen concentration in the upper ∼120 nm thick layer was less than 1 at.%.

The grazing incidence X-ray diffractograms of samples A1–A5 and C are shown in Fig. 2. It can be seen that films A1 and A2 consisted of a mixture of anatase and rutile phases, while the others were pure anatase. In samples A1 and A2, the formation of TiO_2 occurred mainly through the reaction between $TiCl_4$ and H_2O, which caused the growth of both anatase and rutile phases. When the oxidation of TiN contributed more to the formation of TiO_2 during deposition, anatase phase was favoured. It should also be noted that rutile phase existed only in the samples where Ti–N bonding was not detected by XPS (samples A1 and A2). The films A1–A4 also seemed to be slightly (0 0 1) textured. This can be seen most clearly in the case of film A3. Normally, the (1 0 1) reflection is the most intense one in anatase structure but this is not the case here. The unique film growth process, where TiN and TiO_2 deposition pulses alternate, is apparently somehow responsible for this texturing effect. The (0 0 1) texture

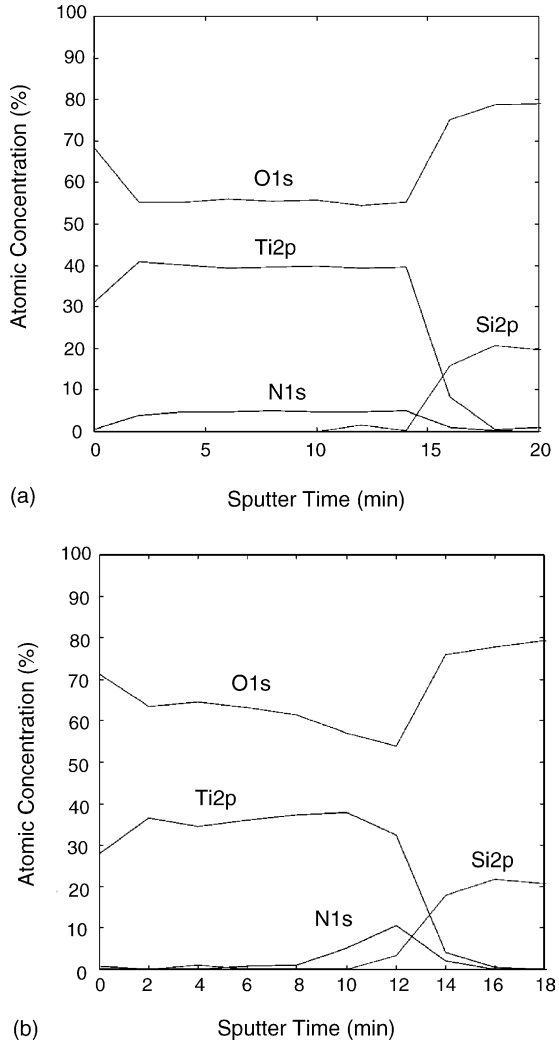

Fig. 1. XPS depth profiles of films (a) B and (b) C.

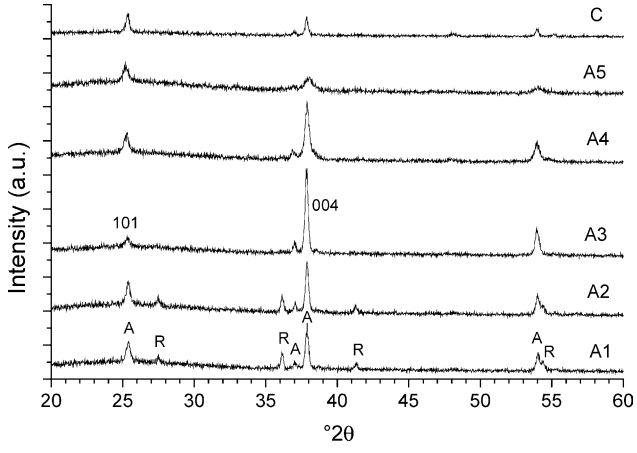

Fig. 2. Grazing incidence XRD patterns of films A1–A5 and C: A, anatase; R, rutile.

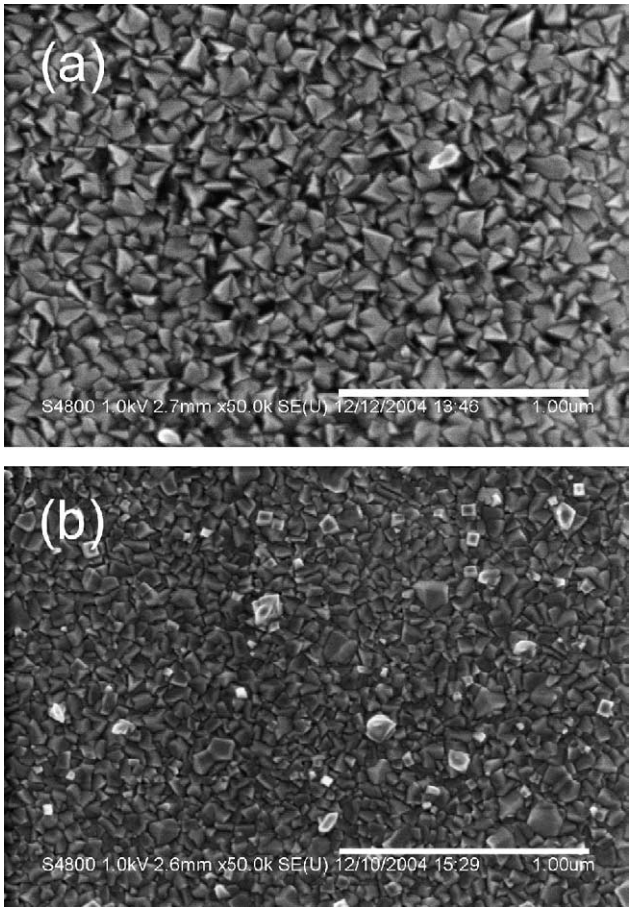

Fig. 3. Scanning electron micrographs of (a) an undoped TiO_2 film and (b) film A3.

of the films was also seen in the θ–2θ scans in which the effect was even more pronounced. The diffractogram of sample B is not shown in Fig. 2 but it was very similar to that of sample A4.

The effect of nitrogen doping on film morphology can be seen from the scanning electron micrographs in Fig. 3. The films look dense and the crystallites are easily seen. The average grain size appears smaller in the nitrogen-doped sample A3 (Fig. 3b) as compared to the undoped one (Fig. 3a). Also, the aforementioned texturing of sample A3 can be seen with some of the rectangular (0 0 1) crystal faces clearly visible.

The grazing incidence X-ray diffractograms of the as-deposited and air-annealed TiN films are shown in Fig. 4. It can be seen that 1-h annealing at 500 °C is not enough to complete the phase conversion from TiN to TiO_2 but results in a mixture of these. Complete phase conversion was achieved in 5 h. It is interesting that at atmospheric pressure the oxidation of TiN produced rutile TiO_2, whereas at reduced pressure in the ALD reactor (∼10 mbar) anatase phase was formed (Fig. 2).

The transmittance spectra of the nitrogen-doped TiO_2 films are shown in Fig. 5. Films A1 and A2, which contained a mixture of anatase and rutile phases, had their absorption edges at a slightly longer wavelength than film A3. This can

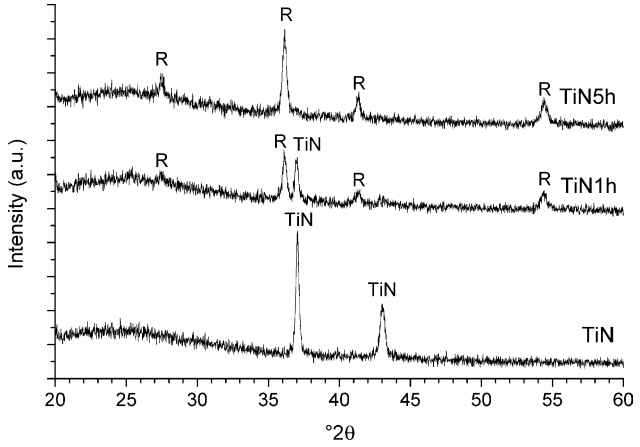

Fig. 4. Grazing incidence XRD patterns of as-deposited and air-annealed TiN films: R, rutile.

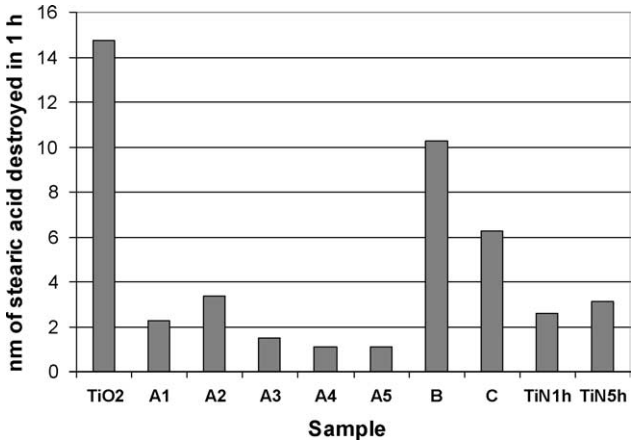

Fig. 6. Decrease of stearic acid layer thickness after 1 h of UV irradiation on TiO_2 and $TiO_{2-x}N_x$ films.

be explained by the absorption of rutile which has a smaller band gap than anatase. Nitrogen doping concentration in the anatase film A3 was not enough to cause a clear increase in visible light absorption. Films A4 and A5, on the other hand, absorbed significantly more visible light. This result is expected from the increased amount of nitrogen in the films. The band gap energies of films A1–A5 were estimated [34] by plotting $(\alpha h\nu)^{1/2}$ versus E (inset of Fig. 5) and are listed in Table 2. The band gap energies of films A1–A3 are higher than the bulk value (3.2 eV) of anatase which is probably the result of quantum size effects. The band gap energies of films A4 and A5 seem to have decreased as a result of nitrogen doping through the mixing of N 2p and O 2p states. At smaller nitrogen concentrations the mixing does not supposedly occur but nitrogen instead forms isolated states just above the valence band [12]. These are the states that have been recognized as the origin of visible light activity in nitrogen-doped TiO_2 [12,16,37,38]. They do not, however, affect the band gap estimation and cannot be seen clearly from the transmittance spectra because of the small thickness and large interference fringes of the films.

3.3. Photocatalytic activity

The results of the stearic acid degradation tests under UV light illumination are shown in Fig. 6. The activities of the nitrogen-doped samples A1–A5 are all weak as compared to undoped TiO_2. With samples A2–A5 the photocatalytic activity decreases with increasing nitrogen concentration. Nitrogen doping by the present method can thus be regarded as detrimental to photocatalytic activity.

Samples B and C had much better activities under UV light than the other nitrogen-doped samples. Both of these films had undoped TiO_2 surface layers which is clearly the reason for the better activity. It is also possible that in these two samples there was enhanced charge separation because of their layered and graded structures. Possible impurity states below the conduction band edge of nitrogen-doped TiO_2 might have acted as traps for electrons photogenerated in the topmost undoped TiO_2 layer [37]. The photogenerated holes would thus have had a longer lifetime and an increased probability to reach the surface before recombination. The stearic acid

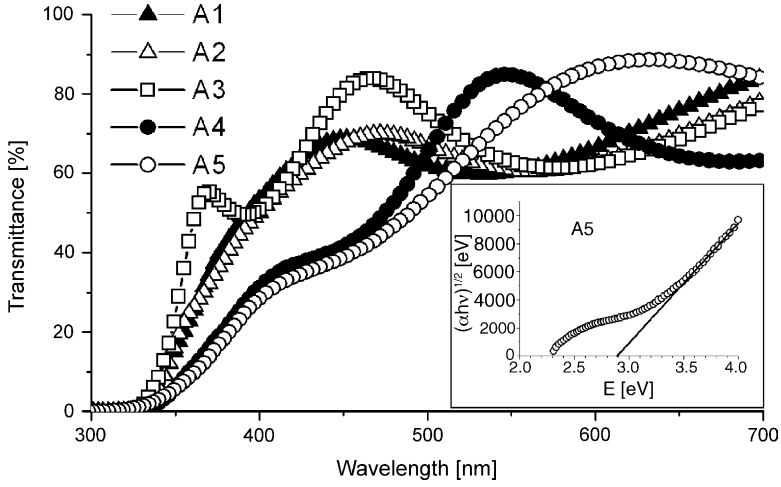

Fig. 5. Transmittance spectra of films A1–A5. Inset: band gap estimation of film A5.

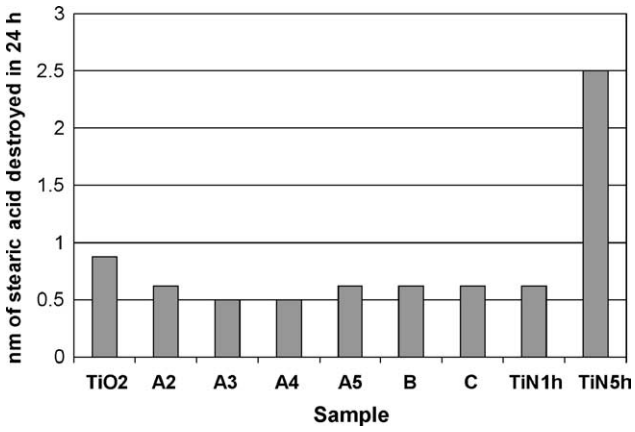

Fig. 7. Decrease of stearic acid layer thickness after 24 h of visible light irradiation on TiO_2 and $TiO_{2-x}N_x$ films.

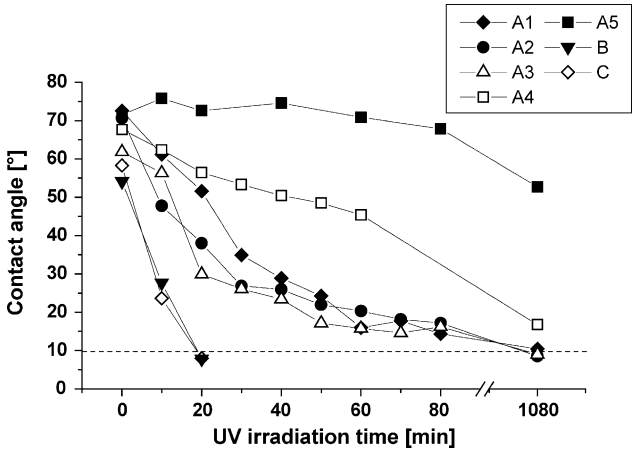

Fig. 8. Change of water contact angle under UV irradiation on $TiO_{2-x}N_x$ films.

degradation rate of more than 10 nm/h of sample B is quite high, considering that the thickness of the undoped layer of this sample is only ~25 nm. An undoped TiO_2 film of 25 nm thickness was found to degrade stearic acid at a rate of 5 nm/h under UV light.

The photocatalytic activities under UV light of the $TiO_{2-x}N_x$ films prepared by annealing TiN in air at 500 °C are also shown in Fig. 6. These samples had low activities, probably because the crystal structure of TiO_2 in these films was rutile (Fig. 4), which is generally known to be photocatalytically much less active than anatase. Sample TiN1h most likely consisted of a layer of TiN with a $TiO_{2-x}N_x$ layer on top [36]. Sample TiN5h, on the other hand, consisted of a single $TiO_{2-x}N_x$ layer. The oxide thickness in sample TiN1h seemed to be already sufficient, because the activities of these two samples were almost equal.

The results of the degradation tests under visible light are shown in Fig. 7. Only the sample which was prepared by annealing TiN in air at 500 °C for 5 h was able to degrade stearic acid under visible light. The other samples did not function under visible light even though they showed a 0.5–1.0 nm change in stearic acid thickness. This small change is not related to photocatalytic degradation, because the same change was detected when stearic acid-coated glass slides were irradiated with visible light. Instead, the observed change is somehow related to the test setup. The results, however, are not affected much because all the samples were subjected to the same conditions and the observed change in stearic acid thickness was always between 0.5 and 1.0 nm.

The effect of post annealing to photocatalytic activity was studied on samples A1–A4. The films were annealed in air at 500 °C for 1 h after which their photocatalytic activities under UV and visible light were examined. The annealing did not cause any noticeable change in the photocatalytic activities.

3.4. Photoinduced superhydrophilicity

Photoinduced superhydrophilicity is an important property of TiO_2 and good results have been reported for $TiO_{2-x}N_x$ also [8]. The wetting properties of the films were studied by measuring their contact angles with water as a function of UV or visible light irradiation. None of the samples became superhydrophilic (contact angle below 10°) when visible light was used for irradiation. However, when UV light was used some samples did show superhydrophilic behaviour (Fig. 8). Only 20 min of irradiation was needed for samples B and C to turn superhydrophilic whereas samples A1–A3 required a much longer time. Samples A4 and A5 did not turn superhydrophilic during the 1080 min irradiation time although their contact angles did decrease. From these results it is obvious that nitrogen in the films seriously weakened their photoinduced superhydrophilicity. Samples B and C turned superhydrophilic rapidly because their surface layers consisted of undoped TiO_2. The reason for the detrimental effect of nitrogen to photoinduced superhydrophilicity is unknown but the results correlate reasonably well with the results of the photocatalytic activity tests.

3.5. Photoelectrochemical measurements

A series of linear sweep voltammograms were measured with undoped and nitrogen-doped TiO_2 films grown on ITO substrates. Fig. 9 shows the current density–voltage plots measured under chopped visible light irradiation in 0.1 M KCl aqueous solution. It can be seen that there was a clear response to visible light irradiation in the nitrogen-doped samples. The appearance of a photocurrent under visible light with films prepared similar to samples A2 and A3 suggests that there are isolated nitrogen-induced states in the band gap because the band gap energies of these samples were 3.3 and 3.4 eV, respectively. The largest photocurrent was observed with a film prepared similar to sample A3 (Fig. 9c). There are, however, features in the voltammograms which indicate that increased recombination is taking place in the $TiO_{2-x}N_x$ films. The appearance of sharp transient spikes when the lamp is switched on and off is one of these, as reported by Lindquist et al. [19,37]. Also, the steady increase

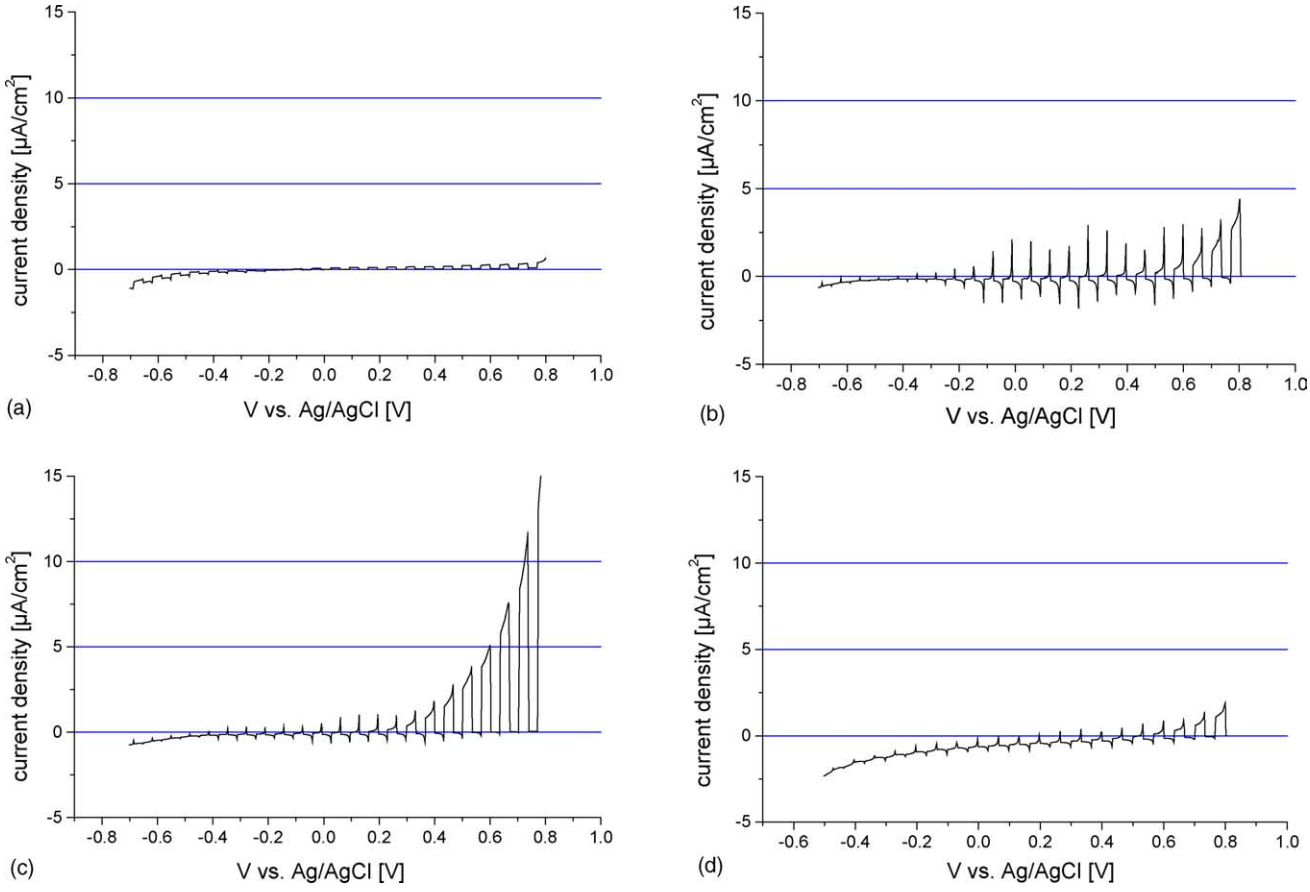

Fig. 9. Linear sweep voltammograms under chopped visible light irradiation of films (a) TiO_2; (b) A2; (c) A3; and (d) A4. The scanning direction was from positive to negative potentials.

of photocurrent when going to more positive potentials is a sign of high recombination rate [19]. A more detailed photoelectrochemical investigation of ALD grown $TiO_{2-x}N_x$ films will be published elsewhere (M. Heikkilä, V. Pore, M. Ritala, M. Leskelä, unpublished results).

It has been reported that nitrogen doping can cause unwanted energy states in the band gap of TiO_2 in addition to those above the valence band edge [37]. These unwanted states can act as recombination centres for photogenerated electron–hole pairs. The recombination centres can be in the form of oxygen vacancies, which create states in the band gap at 0.75–1.18 eV below the conduction band edge [16]. It is known that oxygen vacancies are easily created in wide band gap materials by nitrogen doping due to ionic charge compensation [39,40]. The vacuum in the ALD reactor and the reducing nature of NH_3 gas might have also increased the amount of oxygen vacancies [12,29]. Earlier studies have shown that annealing ALD grown TiO_2 films at 500 °C in air fills a major part of the oxygen vacancies [29]. The fact that air annealing did not have any effect on the photocatalytic activities of samples A1–A4 suggests that the oxygen vacancies do not play a major role in the activity of these samples. Another possibility is that the oxygen vacancies are harder to fill in nitrogen-doped TiO_2 and would have required a higher temperature.

Holes created in the nitrogen-induced states above the valence band by visible light irradiation have smaller mobilities than valence band holes created by UV light [16,37]. This effect combined with a high recombination rate is probably the reason why stearic acid was not decomposed under visible light by samples A1–A5. The origin of the high recombination is still unclear but it must be somehow related to the doping process. One possible explanation for the increased recombination might be the (0 0 1) texture of the films, although, to our knowledge, such an effect has never been reported. Samples B and C had surface layers of undoped TiO_2 which made them active in UV but not in visible light. Sample TiN5h, on the other hand, was able to decompose stearic acid under visible light. Presumably the oxidation of TiN to nitrogen-doped TiO_2 created fewer recombination centres and degradation of stearic acid under visible light was possible. Visible light active $TiO_{2-x}N_x$ films can thus be prepared by ALD of TiN and subsequent anneal in an oxygen containing atmosphere. Higher activities are to be expected by optimising the TiN growth and annealing conditions.

4. Conclusions

This study shows that ALD can be used in the preparation of nitrogen-doped TiO_2 films which are excited by visible light. However, the films prepared in this work using $TiCl_4$, NH_3 and water as precursors suffered from high recombination which lowered the photocatalytic activity under UV light substantially and destroyed the visible light activity completely. Photoinduced superhydrophilicity was also weakened by nitrogen doping. Only the reference $TiO_{2-x}N_x$ sample which was prepared by annealing ALD grown TiN in air was able to decompose stearic acid under visible light. The use of different film deposition parameters or precursors could lead to lower recombination and better photocatalytic activities in the as-deposited films and is currently under investigation.

Acknowledgements

We thank Dr. Marianna Kemell for performing the SEM studies. This work is a part of the technology programme Clean Surfaces 2002–2006 supported by the Finnish National Technology Agency (TEKES).

References

[1] A. Fujishima, K. Honda, Nature 238 (1972) 37.
[2] I. Nakamura, N. Negishi, S. Kutsuna, T. Ihara, S. Sugihara, K. Takeuchi, J. Mol. Catal. A: Chem. 161 (2000) 205.
[3] X.Z. Li, F.B. Li, C.L. Yang, W.K. Ge, J. Photochem. Photobiol. A: Chem. 141 (2001) 209.
[4] Y. Bessekhouad, D. Robert, J.V. Weber, J. Photochem. Photobiol. A: Chem. 163 (2004) 569.
[5] H. Yamashita, Y. Ichihashi, M. Takeuchi, S. Kishiguchi, M. Anpo, J. Synchrotron Radiat. 6 (1999) 451.
[6] M. Anpo, M. Takeuchi, K. Ikeue, S. Dohshi, Curr. Opin. Solid State Mater. Sci. 6 (2002) 381.
[7] T. Umebayashi, T. Yamaki, H. Itoh, K. Asai, J. Phys. Chem. Solids 63 (2002) 1909.
[8] R. Asahi, T. Morikawa, T. Ohwaki, K. Aoki, Y. Taga, Science 293 (2001) 269.
[9] S.U.M. Khan, M. Al-Shahry, W.B. Ingler, Science 297 (2002) 2243.
[10] S. Sakthivel, H. Kisch, Angew. Chem. Int. Ed. 42 (2003) 4908.
[11] T. Umebayashi, T. Yamaki, H. Itoh, K. Asai, Appl. Phys. Lett. 81 (2002) 454.
[12] H. Irie, Y. Watanabe, K. Hashimoto, J. Phys. Chem. B 107 (2003) 5483.
[13] C. Burda, Y. Lou, X. Chen, A.C.S. Samia, J. Stout, J.L. Gole, Nano Lett. 3 (2003) 1049.
[14] J.L. Gole, J.D. Stout, C. Burda, Y. Lou, X. Chen, J. Phys. Chem. B 108 (2004) 1230.
[15] T. Sano, N. Negishi, K. Koike, K. Takeuchi, S. Matsuzawa, J. Mater. Chem. 14 (2004) 380.
[16] M. Miyauchi, A. Ikezawa, H. Tobimatsu, H. Irie, K. Hashimoto, Phys. Chem. Chem. Phys. 6 (2004) 865.
[17] Y. Suda, H. Kawasaki, T. Ueda, T. Oshima, Thin Solid Films 453–454 (2004) 162.
[18] T. Morikawa, R. Asahi, T. Ohwaki, K. Aoki, Y. Taga, Jpn. J. Appl. Phys. 40 (2001) L561.
[19] T. Lindgren, J.M. Mwabora, E. Avendaño, J. Jonsson, A. Hoel, C.-G. Granqvist, S.-E. Lindquist, J. Phys. Chem. B 107 (2003) 5709.
[20] J.-M. Chappé, N. Martin, J.F. Pierson, G. Terwagne, J. Lintymer, J. Gavoille, J. Takadoum, Appl. Surf. Sci. 225 (2004) 29.
[21] S.-Z. Chen, P.-Y. Zhang, D.-M. Zhuang, W.-P. Zhu, Catal. Commun. 5 (2004) 677.
[22] M. Leskelä, M. Ritala, Thin Solid Films 409 (2002) 138.
[23] M. Ritala, M. Leskelä, in: H.S. Nalwa (Ed.), Handbook of Thin Film Materials, vol. 1, Academic Press, New York, 2002, pp. 103–159.
[24] M. Lindblad, S. Haukka, A. Kytökivi, E.-L. Lakomaa, A. Rautiainen, T. Suntola, Appl. Surf. Sci. 121–122 (1997) 286.
[25] M. Ritala, M. Leskelä, E. Nykänen, P. Soininen, L. Niinistö, Thin Solid Films 225 (1993) 288.
[26] M. Ritala, M. Leskelä, L. Niinistö, P. Haussalo, Chem. Mater. 5 (1993) 1174.
[27] M. Ritala, M. Leskelä, E. Rauhala, Chem. Mater. 6 (1994) 556.
[28] K. Kukli, M. Ritala, M. Schuisky, M. Leskelä, T. Sajavaara, J. Keinonen, T. Uustare, A. Hårsta, Chem. Vap. Deposition 6 (2000) 303.
[29] V. Pore, A. Rahtu, M. Leskelä, M. Ritala, T. Sajavaara, J. Keinonen, Chem. Vap. Deposition 10 (2004) 143.
[30] M. Ritala, M. Leskelä, E. Rauhala, P. Haussalo, J. Electrochem. Soc. 142 (1995) 2731.
[31] M. Ritala, M. Leskelä, E. Rauhala, J. Jokinen, J. Electrochem. Soc. 145 (1998) 2914.
[32] T. Suntola, Thin Solid Films 216 (1992) 84.
[33] M. Ylilammi, T. Ranta-aho, Thin Solid Films 232 (1993) 56.
[34] R. Swanepoel, J. Phys. E: Sci. Instrum. 16 (1983) 1214.
[35] P. Sawunyama, L. Jiang, A. Fujishima, K. Hashimoto, J. Phys. Chem. B101 (1997) 11000.
[36] N.C. Saha, H.G. Tompkins, J. Appl. Phys. 72 (1992) 3072.
[37] G.R. Torres, T. Lindgren, J. Lu, C.-G. Granqvist, S.-E. Lindquist, J. Phys. Chem. B 108 (2004) 5995.
[38] R. Nakamura, T. Tanaka, Y. Nakato, J. Phys. Chem. B 108 (2004) 10617.
[39] E.-C. Lee, Y.-S. Kim, Y.-G. Jin, K.J. Chang, Phys. Rev. B 64 (2001) 085120.
[40] O. Diwald, T.L. Thompson, E.G. Goralski, S.D. Walck, J.T. Yates Jr., J. Phys. Chem. B 108 (2004) 52.